Title

Multisite phosphorylation by Cdk1 initiates delayed negative feedback to control mitotic transcription

Journal

Current Biology, 32(1)

ISSN

0960-9822

Authors

Asfaha, Jonathan B
Örd, Mihkel
Carlson, Christopher R
et al.

Publication Date

2022

DOI

10.1016/j.cub.2021.11.001

Peer reviewed

Published in final edited form as:

Curr Biol. 2022 January 10; 32(1): 256–263.e4. doi:10.1016/j.cub.2021.11.001.

Multisite phosphorylation by Cdk1 initiates delayed negative feedback to control mitotic transcription

Jonathan B. Asfaha[1], **Mihkel Örd**[2], **Christopher R. Carlson**[1], **Ilona Faustova**[2], **Mart Loog**[2], **David O. Morgan**[1,*]

[1]Department of Physiology, University of California, San Francisco, San Francisco, USA

[2]Institute of Technology, University of Tartu, Tartu, Estonia

Summary

Cell-cycle progression is driven by the phosphorylation of cyclin-dependent kinase (Cdk) substrates[1-3]. The order of substrate phosphorylation depends in part on the general rise in Cdk activity during the cell cycle[4-7], together with variations in substrate docking to sites on associated cyclin and Cks subunits[3,6,8-10]. Many substrates are modified at multiple sites to provide more complex regulation[10-14]. Here, we describe an elegant regulatory circuit based on multisite phosphorylation of Ndd1, a transcriptional co-activator of budding yeast genes required for mitotic progression[11,12]. As cells enter mitosis, Ndd1 phosphorylation by Cdk1 is known to promote mitotic cyclin (*CLB2*) gene transcription, resulting in positive feedback[13-16]. Consistent with these findings, we show that low Cdk1 activity promotes *CLB2* expression at mitotic entry. We also find, however, that when high Cdk1 activity accumulates in a mitotic arrest, *CLB2* expression is inhibited. Inhibition is accompanied by Ndd1 degradation, and we present evidence that degradation is triggered by multisite Ndd1 phosphorylation by high mitotic Cdk1-Clb2 activity. Complete Ndd1 phosphorylation by Clb2-Cdk1-Cks1 requires the phosphothreonine-binding site of Cks1, as well as a recently identified phosphate-binding pocket on the cyclin Clb2[17]. We therefore propose that initial phosphorylation by Cdk1 primes Ndd1 for delayed secondary phosphorylation at suboptimal sites that promote degradation. Together, our results suggest that rising levels of mitotic Cdk1 activity act at multiple phosphorylation sites on Ndd1, first triggering rapid positive feedback and then promoting delayed negative feedback, resulting in a pulse of mitotic gene expression.

eTOC blurb

*Lead Contact: David.Morgan@ucsf.edu.

Author contributions

J.B.A. conceived the project, performed experiments and analyzed results, with assistance from C.R.C. and guidance from D.O.M. and M.L. M.Ö., I.F., and M.L. performed Ndd1 phosphorylation analyses in vitro. J.B.A. and D.O.M. wrote the paper with assistance from all other authors.

Declaration of interests

The authors declare no competing interests.

Asfaha et al. demonstrate that the protein kinase Cdk1 limits mitotic gene expression by promoting degradation of the transcriptional co-activator Ndd1. Ndd1 degradation is triggered by a complex pattern of phosphorylation events that depend in part on phosphate binding by the cyclin and Cks subunits associated with Cdk1.

Graphical Abstract

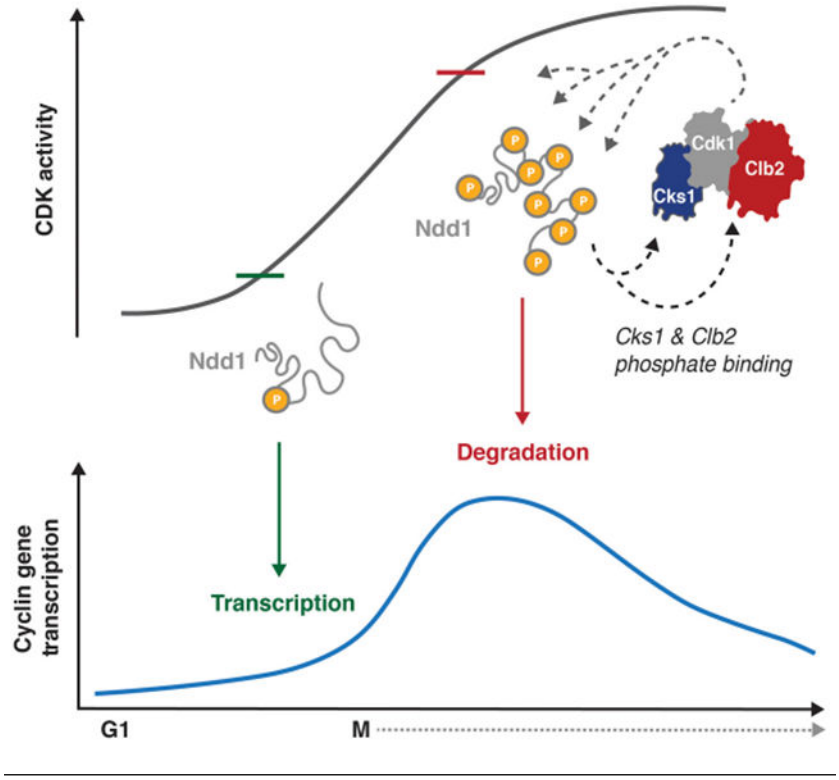

Results and Discussion

Negative feedback suppresses mitotic gene expression in a mitotic arrest

We used RT-qPCR to measure the expression of the *CLB2* cluster of mitotic genes[12] in the budding yeast *Saccharomyces cerevisiae*. As in previous studies, we found that expression of genes in this cluster reaches peak levels in mitosis, 60 min after release from a G1 arrest (Figure 1A)[12]. Transcriptional activation is driven by M-phase Cdk1 activity[4,18,19] We therefore expected that high Cdk1 activity in a mitotic arrest would sustain continuous transcription of mitotic genes. To test this possibility, we arrested cells in G1 and released them into nocodazole, a microtubule poison that activates the spindle assembly checkpoint and arrests cells in mitosis. Surprisingly, we found that upon entry into a mitotic arrest, expression of mitotic genes decreased to between 50% and 20% of peak levels (Figure 1B). Similar results were obtained when cells were arrested in mitosis by *CDC20* depletion, indicating that the effect was not due to spindle assembly checkpoint activation (Figure 1C).

Despite the reduction in transcript levels, Clb2 protein levels remained at a constant high level in a mitotic arrest, as seen in previous studies (Figure 1D)[20-22]. Clb2 is very stable in

a mitotic arrest, which would explain its high steady-state levels despite the decline in its mRNA transcript.

Cdk1-mediated positive feedback promotes *CLB2* transcriptional activation in mitosis[14,15,19,23]. We hypothesized that high mitotic Cdk1 activity might suppress *CLB2* transcription. We inhibited Cdk1 at various inhibitor concentrations in an analog-sensitive Cdk1 mutant, *cdk1-as1*. Cdk1 in this strain bears an F88G mutation in the active site, making Cdk1 highly selective for the inhibitor 1-NM-PP1[24] Mild Cdk1 inhibition, at 50 nM or 100 nM 1-NM-PP1, delayed the reduction in *CLB2* transcription (Figure 1E). Mild inhibition did not significantly affect the initial mitotic rise in *CLB2* expression, suggesting that partial Cdk1 inhibition did not affect transcriptional activation. However, strong Cdk1 inhibition, at 250 nM or 500 nM 1-NM-PP1, suppressed transcription (Figure 1F). Thus, strong Cdk1 inhibition inhibits positive feedback and transcriptional activation, while mild inhibition blocks negative feedback while leaving positive feedback less affected. A simple explanation for these results is that negative feedback requires higher levels of kinase activity and is therefore more readily inhibited by partial kinase inhibition.

Ndd1 is destabilized in a mitotic arrest by N-terminal phosphorylation sites

Ndd1 is a key positive regulator of the *CLB2* transcriptional cluster and is activated by Cdk1-mediated phosphorylation[15]. We therefore tested its role in the negative feedback we observed. Immunoblotting revealed that Ndd1 levels decreased as cells proceeded into a mitotic arrest from G1, and this decline could be alleviated by the addition of 100 nM 1-NM-PP1 (Figure 2A, Figure S1A).

We measured the effect of Cdk1 inhibition on Ndd1 stability at various points after release from G1. We estimated Ndd1 half-life by measuring its decline after addition of cycloheximide at 60, 90, or 150 min after release from G1 into a mitotic arrest. We found that Ndd1 degradation rate increased as cells proceeded into the mitotic arrest (Figure 2B; blue). Inhibition of Cdk1 with 500 nM 1-NM-PP1 prevented Ndd1 degradation at all time points (Figure 2B; red). These data indicate that Cdk1-dependent Ndd1 degradation rate increases gradually during a mitotic arrest, suggesting that prolonged high Cdk1 activity promotes degradation.

Ndd1 contains 16 Cdk1 consensus phosphorylation sites (minimal site: S/T-P; full site: S/T-P-x-K/R), most of which are conserved in budding yeasts (Figure 2C, Figure S2). Mutation of all 16 sites is known to stabilize Ndd1 in a spindle checkpoint arrest[25]. To identify the specific sites in Ndd1 that are required for degradation, we first assessed the stability of Ndd1 truncation mutants. Deletion of the amino-terminal 115 amino acids stabilized Ndd1 (Figure 2C). Two minimal Cdk1 consensus sites, S47 and T57, are found in this region. Consistent with the importance of these sites, an S47A substitution partially stabilized Ndd1, while a T57A substitution led to a greater level of stabilization (Figure 2D, Figure S1B).

Mutation of all 16 Cdk1 sites (the Ndd1-16A mutant) resulted in greater Ndd1 stabilization than that seen with the T57A mutant (Figure 2E, blue; Figure S1C). Adding back S47 and T57 to the 16A mutant did not induce degradation (Figure 2E, red; Figure S1C). Thus, S47 and T57 are required but not sufficient for rapid Ndd1 degradation.

Ndd1 is required for high mitotic *CLB2* transcription[15], and therefore Ndd1 degradation is likely to be responsible, at least in part, for the decline in *CLB2* transcription during a mitotic arrest. We tested the importance of Ndd1 degradation by analyzing *CLB2* mRNA levels in a yeast strain in which *NDD1* was replaced with a mutant gene encoding Ndd1-T57A. When cells expressing this mutant protein were released from a G1 arrest into nocodazole, Ndd1-T57A protein levels remained high (Figure 2F). This mutant did not affect the initial rate of increase in *CLB2* transcription or the timing of the peak of maximum transcription. *CLB2* mRNA levels accumulated to higher levels in the mutant strain (Figure 2G), but a gradual decline in *CLB2* mRNA was still apparent. Thus, although Ndd1 degradation contributes to decreased *CLB2* transcription, additional mechanisms are also involved. For example, Cdk1-mediated phosphorylation at certain sites in Ndd1 could interfere with its co-activator function, or transcriptional inhibition might be due in part to phosphorylation of other transcriptional regulators, such as Fkh2.

Our work suggests that early Cdk1 activity at the *CLB2* promoter stimulates the production of Clb2-Cdk1 activity as cells enter mitosis, after which accumulation of high Clb2-Cdk1 activity leads to delayed negative feedback that inhibits transcription, in part through Ndd1 degradation and in part through other, as yet unidentified, mechanisms. This time-delayed negative feedback system generates a pulse of mitotic transcription in a mitotic arrest[26].

Ndd1 degradation depends on multiple Clb2-dependent phosphorylation sites

Because S47 and T57 are not sufficient to induce degradation, and their mutation does not fully stabilize Ndd1, we searched for other sites that contribute to Ndd1 destabilization. We systematically added back clusters of predicted Cdk1 sites to Ndd1-16A, starting at the amino terminus, and measured the stability of each mutant (Figure 3A). Adding back predicted Cdk1 sites up to and including T236 (the Ndd1-8A mutant) had minimal effects on degradation rate (Figure 3B). However, further addition of S254 and T265 (the Ndd1-6A mutant) led to a decline in stability (Figure 3C). Addition of more predicted C-terminal Cdk1 sites further destabilized the protein (Figure 3C).

We added back either S254 or T265 to Ndd1-8A. Addition of either site led to an intermediate level of destabilization that fell between those of Ndd1-8A and Ndd1-6A (Figure 3D, Figure S3A). Thus, both sites promote instability. Interestingly, however, when S254 and T265 are both mutated to alanine in an otherwise wild-type protein, Ndd1 is not stabilized (Figure 3E, Figure S3B). Furthermore, a version of Ndd1 that contains only S47, T57, S254, and T265 is stable (Figure 3F, Figure S3C), showing that these four sites, despite their contributions in some contexts, are not sufficient for degradation. Finally, a mutant containing only T57, S254, T265, and all sites C-terminal of T265, was partially destabilized (Figure 3G, Figure S3D), consistent with evidence in Figure 3C that sites C-terminal of T265 are sufficient to promote some degradation. Together, our studies of numerous site mutations suggest that multiple sites collaborate to induce Ndd1 degradation.

If Ndd1 stability is tied to cell cycle stage, then cyclin specificity may be an important determinant of Ndd1 destruction. The two major mitotic cyclins, Clb3 and Clb2, are thought to act in sequence as cells approach and progress into mitosis, so we tested their contributions to Ndd1 stability in a mitotic arrest. Deletion of Clb3 had no effect, whereas

deletion of Clb2 increased the stability of Ndd1 (Figure 3H). Thus, Ndd1 instability depends primarily on high Clb2-dependent Cdk1 activity during a prolonged mitotic arrest.

To gain more insight into the roles of specific sites, we used mass spectrometry to identify major Cdk1-dependent phosphorylation sites in vitro. Previous biochemical studies have demonstrated that Ndd1 is an excellent substrate of both Clb3-Cdk1 and Clb2-Cdk1[27-29]. We confirmed that purified Clb2-Cdk1-Cks1 complexes phosphorylate multiple sites in Ndd1, with some preference for S254 and other sites in the amino-terminal region (Figure S4A). We also compared the rates of phosphorylation by Clb2-Cdk1-Cks1 and Clb3-Cdk1-Cks1 at specific sites (Figure S4B). We observed moderate Clb3 specificity for sites C-terminal of T277, including T319, which is required for Ndd1 activation[15]. In the amino-terminal half of the protein, T265 displayed moderate Clb2 specificity. Unfortunately, phosphorylation at the two key N-terminal sites, S47 and T57, was not measurable in these experiments because the peptide containing these sites was not detected in the mass spectrometer (Figure S4C). We therefore turned to other methods for analysis of these sites, as described next.

Phosphorylation of N-terminal sites depends on priming by phosphate-binding sites in Cks1 and Clb2

The requirement for multiple phosphorylation sites for Ndd1 degradation is reminiscent of other Cdk1 substrates, including the Cdk1 inhibitor Sic1. Sic1 degradation depends on the ubiquitin ligase SCF^{Cdc4}, which interacts directly with short phosphorylated sequence motifs (phosphodegrons) on Sic1. Interestingly, many phosphorylation sites in Sic1 are destabilizing because they act as priming sites to stimulate secondary phosphorylation at a phosphodegron. These mechanisms depend on the phosphothreonine-binding site of the Cdk-associated Cks1 subunit, which interacts with priming phosphorylation sites to promote phosphorylation at other sites[6,9,29,30].

With these ideas in mind, we used Phos-tag SDS-PAGE to analyze Ndd1 phosphorylation by Cdk1 in vitro[31]. To improve gel resolution, we used a truncated protein containing the N-terminal 272 residues, which contains ten Cdk1 sites, including those most clearly implicated in degradation (S47, T57, S254, T265). Ndd1 is predicted to be disordered, so truncation is unlikely to disrupt a folded domain. Phosphorylation by wild-type Clb2-Cdk1-Cks1 led to phosphorylation of many sites on this protein (Figure 4A; panel 1). Mutation of S47 and T57 greatly reduced the formation of hyperphosphorylated Ndd1, demonstrating that one or both of these sites are substrates of Clb2-Cdk1-Cks1. The S47A T57A mutations had little effect on the hypophosphorylated forms seen at earlier time points in the reaction, indicating that S47 and T57 are phosphorylated at a lower rate than several rapidly phosphorylated initial sites.

Mutation of the phosphothreonine-binding pocket of Cks1 greatly reduced the hyperphosphorylated Ndd1 forms, but had a minor impact on the primary phosphorylation sites at early time points (Figure 4A; panel 2). S47A T57A mutations further reduced the hyperphosphorylated forms but had little effect on rapidly phosphorylated forms. Cks1 therefore enhances phosphorylation of multiple weaker sites, including S47 and T57.

Recent structural studies led to the discovery of a previously uncharacterized phosphate-binding pocket on the surface of human cyclin B1[17]. The three basic residues that form this pocket are highly conserved throughout the eukaryotic B-type cyclins and are found in all six of the budding yeast Clb proteins. We hypothesized that this pocket in Clb2 might act, like Cks1, to enhance phosphorylation of Ndd1 following phosphorylation at priming sites. Consistent with this idea, we found that mutation of the three key residues in the Clb2 pocket (R366A R379A K383A, termed Clb2-PP) reduced Ndd1 phosphorylation, particularly at sites modified at later time points (Figure 4A; panel 3). Mutation of S47 and T57 reduced phosphorylation at these sites further. The Clb2 phosphate-binding pocket was also required for full phosphorylation of full-length Ndd1 (Figure 4B).

When we combined mutations in the phosphate-binding sites of both Cks1 and Clb2, hyperphosphorylation of Ndd1 was reduced to a level slightly lower than that seen in either single mutant (Figure 4A; panel 4). Mutation of S47 and T57 in this context caused an additional slight reduction.

Together, the results in Figure 4A argue that disruption of phosphate binding by either Cks1 or Clb2 causes a major decline in Ndd1 hyperphosphorylation, while disruption of both sites has only a small additional effect. Thus, extensive hyperphosphorylation requires substrate docking to both phosphate-binding sites.

We compared the patterns of phosphorylation of Ndd1 (1-272) with Clb2 and Clb3. Clb3 was far less effective in catalyzing hyperphosphorylation (Figure 4C). Furthermore, mutations of S47 and T57 had no effect on the pattern of phosphorylation by Clb3-Cdk1-Cks1, indicating that this kinase does not phosphorylate these sites under these conditions. These results are consistent with our evidence that Clb3 does not contribute significantly to Ndd1 degradation in the cell (Figure 3H).

We also used Phos-Tag gels to analyze the phosphorylation state of Ndd1 in the cell. The stable Ndd1-T57A mutant accumulated in a highly phosphorylated form (Figure 4D), as predicted if T57 is a secondary site that is phosphorylated after priming at other sites. In the absence of T57, these other sites do not promote rapid degradation.

Importantly, we also obtained evidence that priming is required for rapid Ndd1 degradation, using a yeast strain in which the *CLB2* gene was replaced with a gene encoding the Clb2-PP mutant. This strain did not display major cell cycle defects, as expected given that *clb2*Δ cells are viable. In nocodazole-arrested cells, steady-state levels of Ndd1 were higher in this strain than in the wild type, and half-life analysis indicated that Ndd1 was partially stabilized in mutant cells (Figure 4E). These results suggest that the phosphate-binding pocket of Clb2 helps promote secondary phosphorylation at sites, such as S47 and T57, that target Ndd1 for degradation.

In total, our studies of the stability of various Ndd1 phosphomutants, together with biochemical analyses of Ndd1 phosphorylation in vitro, suggest that full Ndd1 phosphorylation and degradation depend on sequential cascades of phosphorylation. Rapidly phosphorylated primary sites interact with phosphate-binding sites on Cks1 and Clb2, which leads to delayed, partial secondary phosphorylation at suboptimal sites that promote

degradation. Inside the cell, we speculate that these mechanisms create a system in which degradation occurs only when kinase activity rises above a threshold that overcomes opposing phosphatases acting on the same degradative sites[10,29].

Our work provides evidence that a recently described phosphate-binding pocket on B-type cyclins[17] contributes to the regulation of Cdk1 substrate phosphorylation. Cks1 is known to direct phosphorylation downstream of priming phosphothreonine sites[10,29], but the specificity of the cyclin phosphate-binding pocket is not known. Detailed further studies with an array of Ndd1 mutants will be required to clarify which sites act as priming sites, and whether Cks1 and Clb2 act in sequence or simultaneously in promoting secondary phosphorylation. Additional studies will also be required to assess the role of the cyclin pocket in phosphorylation of other substrates or regulators. There is evidence, for example, that the residues in this pocket influence interactions between cyclin and the regulatory phosphatase Cdc25[32].

The mechanism of Ndd1 degradation remains unclear. Numerous other proteins, including Sic1, are known to be destabilized by Cdk1-mediated phosphorylation, and in many of these cases Cdk1 phosphorylation generates phosphodegron motifs recognized by F-box subunits of the ubiquitin ligase SCF[33-36]. The F-box protein Grr1 is known to be required for Ndd1 degradation in asynchronous cells[25], suggesting that phosphorylated Ndd1 is targeted by the ubiquitin ligase SCF^{Grr1}. Grr1 contains a leucine-rich repeat domain with multiple positively-charged residues that are thought to recognize clusters of phosphosites on Grr1-specific substrates[35], including Cln2 and Hof1[34,37-39]. The simplest explanation for our results is that Grr1 recognizes specific phosphorylation clusters on Ndd1. It remains possible that phosphorylation destabilizes Ndd1 through other mechanisms, such as by affecting Ndd1 localization or its interactions with the transcriptional machinery.

Many of the Cdk1 sites in Ndd1 are grouped into pairs of sites 10-12 residues apart (Figure S2). This spacing is seen for S47/T57 and for S254/T265, which contribute to degradation. Perhaps these pairs serve as weak diphosphodegrons dispersed at multiple locations. Alternatively, the spacing of these residues might serve some role in the priming mechanism by which Cks1 or Clb2 interacts with one site and promotes phosphorylation at another.

If later Clb2-dependent phosphorylation events destabilize Ndd1, then early phosphorylation events, catalyzed by Clb3-Cdk1, are likely to initiate the activation of Ndd1. Indeed, previous studies suggest that *CLB2* transcription is partially reduced in the absence of Clb3[19]. Cdk1-dependent phosphorylation of T319 on Ndd1 is critical for its promoter recruitment and thus for *CLB2* transcriptional activation[15]. Our mass spectrometry studies revealed that T319 displays moderate specificity for Clb3 over Clb2 (Figure S4B), and recent evidence suggests that T319 phosphorylation is reduced in a strain with Clb2 as the only B-type cyclin[7]. Other studies have demonstrated that Ndd1 phosphorylation depends in part on the substrate-docking pocket of Clb3[27]. Clb3 might therefore initiate Ndd1 activation before positive feedback is triggered by Clb2 (and Cdc5[40]). Upon entry into mitosis, Clb2-Cdk1 alone is capable of catalyzing phosphorylation of the key degradative sites in Ndd1,

perhaps due to its higher intrinsic activity[28], its higher concentration in the nucleus[10], or specificity in its phosphate-binding pocket.

Multiple sites in the C-terminal region of Ndd1 enhance the rate of Ndd1 degradation (Figures 3C,G). Some of these sites display moderate Clb3 specificity (Figure S4B), suggesting that early Clb3-dependent C-terminal phosphorylation contributes to Ndd1 degradation as the cell enters mitosis. However, although Clb3 is abundant in nocodazole-arrested cells[22], our results argue that it is not required for Ndd1 degradation in those cells (Figure 3H). Phosphorylation of C-terminal sites by Clb2-Cdk1 appears to be sufficient to enhance degradation in a mitotic arrest.

Hundreds of Cdk1 substrates are phosphorylated at specific times during progression through the cell cycle[1-3]. Many of these proteins contain arrays of phosphorylation sites in disordered regions. The timing and switch-like behavior of phosphorylation are governed by a remarkably complex variety of parameters, including the sequences, affinities, positioning, and distancing of phosphosites and cyclin-specific docking motifs[9]. Ndd1 appears to provide an intriguing case in which multisite phosphorylation of a single protein, by sequential cyclin-Cdk1 complexes, provides ordered activation and inactivation of a specific cell cycle process.

STAR METHODS

RESOURCE AVAILABILITY

Lead contact—Further information and requests for resources and reagents should be directed to and will be fulfilled by the lead contact, David Morgan (david.morgan@ucsf.edu).

Materials availability—Materials generated in this study are available upon request from the lead contact.

Data and code availability

- All data reported in this paper will be shared by the lead contact upon request.
- This paper does not report original code.
- Any additional information required to reanalyze the data reported in this paper available from the lead contact upon request.

EXPERIMENTAL MODEL AND SUBJECT DETAILS

All strains are derivatives of W303a and listed in the Key Resources Table. All strains were constructed using PCR- and/or restriction digest-based homologous recombination. Cells were grown in Yeast Extract Peptone (YEP) containing a combination of Raffinose, Galactose, Dextrose, or a combination thereof. For all experiments, cells were grown at 30°C and progressed through a minimum of two doubling times in log phase before any experiments were performed. For all time courses, cultures reached an $OD_{595\ nm}$ = 0.15–0.3 before synchronization. Cells were synchronized in G1 using 1.5 μg/ml alpha-factor for 3 h

at 30°C and released by washing three times in fresh media. Cells were arrested in mitosis by addition of 15 μg/ml nocodazole for 3 h at 30°C.

METHOD DETAILS

Analysis of gene expression—100 μl total RNA was prepared from 1 ml cultures by hot-acid phenol chloroform extraction. RNA concentration was measured with a NanoDrop spectrophotometer (ThermoFisher Scientific); concentrations of RNA preparations were 300-500 ng/μl. 5% of total RNA was treated with TURBO DNase as follows: 5 μl total RNA was added to 5 μl 10x TURBO DNase reaction buffer, 1 μl TURBO DNase, and 39 μl water. After 30 min at 37°C, DNase was inactivated by addition of 5 μl TURBO DNase inactivating reagent for 5 min at room temperature. RT-qPCR was carried out to manufacturer specifications in a CFX96 Touch Real-Time PCR Machine (Bio-Rad). For each reaction, 5 μl of 2x Luna Universal One-Step Reaction Mix was added to 0.5 μl of 20x Luna WarmStart RT Enzyme Mix, 0.4 μl forward primer, 0.4 μl reverse primer (0.4 μM final concentration for each primer), 1 μl of TURBO DNase-treated RNA, and 2.7 μl water. The RT-qPCR program was set to SYBR/FAM detection mode and the program was executed as follows: Step 1, 55°C for 10 min; Step 2, 95°C for 1 min; Step 3, 95°C for 10 s; Step 4, 60°C for 30 s plus plate read; Step 5, repeat cycle 40x starting at step 3. *CLB2, CDC5, and CDC20* expression were normalized to *ACT1* gene expression[42]. The amplicon was confirmed by melt curve analysis from 60°C to 95°C in 0.5°C increments. Relative expression was calculated by the $2^{-\Delta C_T}$ method[43]. Primers are listed in the Key Resources Table.

Western blotting—Ndd1 stability was analyzed in yeast strains expressing C-terminally Myc-tagged Ndd1 at the endogenous locus or under the control of the *GAL1-10* promoter. In the latter case, *NDD1* expression was induced during mitotic synchronization by the addition of galactose to a final concentration of 2% in YEP-Raffinose. Cycloheximide was added to a final concentration of 250 μg/ml to halt translation, and 1 ml samples were harvested every 10 min to measure Ndd1 levels by western blotting.

For western blotting, yeast lysates were prepared by bead-beating cells in 100 μl urea lysis buffer (20 mM Tris-HCl pH 7.4, 7 M urea, 2 M thiourea, 65 mM CHAPS, 10 mM DTT). Equal volumes of lysates were separated by SDS-PAGE and transferred at a constant voltage of 100V for 1h at 4°C in Tris/Glycine Buffer to a 0.45-micron nitrocellulose membrane (GE-Healthcare Life Sciences). Blots were probed with the following antibodies diluted 1:5000 in TBS-T (10 mM Tris-HCl pH 8.0, 150 mM NaCl, 05% Tween-20) containing 5% (w/v) nonfat dry milk: Mouse anti-Myc, Mouse anti-HA, Rabbit anti-Mouse IgG (H+L) Alexa Fluor 680, or 800CW Donkey anti-Mouse IgG. GAPDH Monoclonal Antibody was diluted 1:1500 in TBS-T containing 5% (w/v) nonfat dry milk. Primary antibodies were incubated overnight at 4°C. Secondary antibodies were incubated at room temperature for 1h. After each incubation, blots were washed for 3 times over 5 min with TBS-T. Fluorescence on the blots was imaged on an Odyssey Fc imager (LI-COR) at 700 nm for 10 min.

Analysis of Ndd1 phosphorylation—6xHis-tagged Ndd1 and Ndd1 (1-272) were expressed from pET28a in *E. coli* BL21RP cells at 30°C using 0.3 mM IPTG. 6xHis-Ndd1

was purified using immobilized nickel affinity chromatography and eluted with imidazole. Clb3- and Clb2-Cdk1 complexes were purified from *S. cerevisiae* lysates using TAP-tagged cyclins as described previously[1,44]. Cks1 was expressed in *E. coli* BL21RP and purified as described[45].

For multisite phosphorylation analysis of Ndd1 and mutants, phosphorylation reactions were supplemented with [γ-^{32}P]-ATP (Hartmann Analytic). Reactions were stopped at 5, 15, 30 and 60 min by pipetting an aliquot into SDS-PAGE sample buffer supplemented with 1 mM $MnCl_2$. Reactions with full-length Ndd1 were separated using Mn-Phos-tag SDS-PAGE with 8% acrylamide and 25 μM Phos-tag (Wako Chemicals). For Ndd1 (1-272), SDS-PAGE with 8% acrylamide and 50 μM Phos-tag was used. ^{32}P phosphorylation signals were detected using an Amersham Typhoon 5 Biomolecular Imager (GE Healthcare Life Sciences) and quantified using ImageQuant TL (Amersham Biosciences).

For mass spectrometry analysis, kinase reactions were carried out at room temperature in 50 mM Hepes- KOH pH 7.4, 150 mM NaCl, 5 mM $MgCl_2$, 20 mM imidazole, 2% glycerol, 0.2 mg/ml BSA, and 500 μM ATP. The concentration of Ndd1 was 1 μM and that of Cks1 was 500 nM. To quantitatively compare the phosphorylation of Ndd1 at different sites in different conditions, the reactions were supplemented with either normal isotopic ATP ([^{16}O]ATP) or heavy ATP ([^{18}O]ATP) (Cambridge Isotope Laboratories). To compare Ndd1 phosphorylation at low initial substrate turnover and high turnover, Ndd1 was phosphorylated with 0.4 nM Clb2-Cdk1 for 4 min for low turnover, or 2 nM Clb2-Cdk1 for 40 min for high turnover. For comparison of phosphorylation by Clb2- and Clb3-Cdk1, 0.4 nM Cdk1 complex was used for 20 min. Reactions were stopped with SDS loading buffer, and aliquots from different reactions were mixed together in a 1:1 ratio and analyzed by SDS-PAGE. The gel was stained with Colloidal Coomassie G-250 and the Ndd1 band was excised. In-gel digestion was performed using trypsin/P (20 ng/μl), and peptides were purified using C18 StageTips. Peptides were separated by an Agilent 1200 series nanoflow system (Agilent Technologies) and analyzed using an LTQ Orbitrap classic mass spectrometer (Thermo Electron) equipped with a nanoelectrospray ion source (Proxeon). Mascot 2.3 (Matrix Science) was used to identify the peptides. Two independent experiments were performed.

QUANTIFICATION AND STATISTICAL ANALYSIS

RT-qPCR and half-life measurements represent means from 2 to 4 independent experiments, and error bars indicate the standard error of the mean. Ndd1 half-life curves were fit to a single exponential decay model in Graphpad Prism Version 9.2.0.

Supplementary Material

Refer to Web version on PubMed Central for supplementary material.

Acknowledgements

We thank members of the Morgan and Loog laboratories for discussions and comments on the manuscript. This work was supported by an HHMI Gilliam Graduate Fellowship (to J.B.A), a grant from the National Institute of General Medical Sciences (R35-GM118053, to D.O.M.), ERC Consolidator Grant 649124 (to M.L.), Centre of

Excellence for Molecular Cell Technologies TK143 (to M.L.), and Estonian Science Agency grant PRG550 (to M.L.).

References

1. Ubersax JA, Woodbury EL, Quang PN, Paraz M, Blethrow JD, Shah K, Shokat KM, and Morgan DO (2003). Targets of the cyclin-dependent kinase Cdk1. Nature 425, 859–864. [PubMed: 14574415]
2. Holt LJ, Tuch BB, Villén J, Johnson AD, Gygi SP, and Morgan DO (2009). Global analysis of Cdk1 substrate phosphorylation sites provides insights into evolution. Science 325, 1682–1686. [PubMed: 19779198]
3. Loog M, and Morgan DO (2005). Cyclin specificity in the phosphorylation of cyclin-dependent kinase substrates. Nature 434, 104–108. [PubMed: 15744308]
4. Swaffer MP, Jones AW, Flynn HR, Snijders AP, and Nurse P (2016). CDK Substrate Phosphorylation and Ordering the Cell Cycle. Cell 167, 1750–1761. [PubMed: 27984725]
5. Coudreuse D, and Nurse P (2010). Driving the cell cycle with a minimal CDK control network. Nature 468, 1074–1079. [PubMed: 21179163]
6. Kõivomägi M, Valk E, Venta R, Iofik A, Lepiku M, Balog ERM, Rubin SM, Morgan DO, and Loog M (2011). Cascades of multisite phosphorylation control Sic1 destruction at the onset of S phase. Nature 480, 128–131. [PubMed: 21993622]
7. Ercan DP, Chrétien F, Chakravarty P, Flynn HR, Snijders AP, and Uhlmann F (2021). Budding yeast relies on G1 cyclin specificity to couple cell cycle progression with morphogenetic development. Sci. Adv 7, eabg0007. [PubMed: 34088668]
8. Bhaduri S, and Pryciak PM (2011). Cyclin-specific docking motifs promote phosphorylation of yeast signaling proteins by G1/S Cdk complexes. Curr. Biol 21, 1615–1623. [PubMed: 21945277]
9. Örd M, Venta R, Möll K, Valk E, and Loog M (2019). Cyclin-Specific Docking Mechanisms Reveal the Complexity of M-CDK Function in the Cell Cycle. Mol. Cell 75, 76–89. [PubMed: 31101497]
10. Örd M, Möll K, Agerova A, Kivi R, Faustova I, Venta R, Valk E, and Loog M (2019). Multisite phosphorylation code of CDK. Nat. Struct. Mol. Biol 26, 649–658. [PubMed: 31270471]
11. Wittenberg C, and Reed SI (2005). Cell cycle-dependent transcription in yeast: promoters, transcription factors, and transcriptomes. Oncogene 24, 2746–2755. [PubMed: 15838511]
12. Spellman PT, Sherlock G, Zhang MQ, Iyer VR, Anders K, Eisen MB, Brown PO, Botstein D, and Futcher B (1998). Comprehensive identification of cell cycle-regulated genes of the yeast Saccharomyces cerevisiae by microarray hybridization. Mol. Biol. Cell 9, 3273–3297. [PubMed: 9843569]
13. Kumar R, Reynolds DM, Shevchenko A, Goldstone SD, and Dalton S (2000). Forkhead transcription factors, Fkh1p and Fkh2p, collaborate with Mcm1p to control transcription required for M-phase. Curr. Biol 10, 896–906. [PubMed: 10959837]
14. Pic-Taylor A, Darieva Z, Morgan BA, and Sharrocks AD (2004). Regulation of cell cycle-specific gene expression through cyclin-dependent kinase-mediated phosphorylation of the forkhead transcription factor Fkh2p. Mol. Cell. Biol 24, 10036–10046. [PubMed: 15509804]
15. Reynolds D, Shi BJ, McLean C, Katsis F, Kemp B, and Dalton S (2003). Recruitment of Thr 319-phosphorylated Ndd1p to the FHA domain of Fkh2p requires Clb kinase activity: a mechanism for CLB cluster gene activation. Genes Dev. 17, 1789–1802. [PubMed: 12865300]
16. Darieva Z, Pic-Taylor A, Boros J, Spanos A, Geymonat M, Reece RJ, Sedgwick SG, Sharrocks AD, and Morgan BA (2003). Cell cycle-regulated transcription through the FHA domain of Fkh2p and the coactivator Ndd1p. Curr. Biol 13, 1740–1745. [PubMed: 14521842]
17. Yu J, Raia P, Ghent CM, Raisch T, Sadian Y, Cavadini S, Sabale PM, Barford D, Raunser S, Morgan DO, et al. (2021). Structural basis of human separase regulation by securin and CDK1–cyclin B1. Nature 596, 138–142. [PubMed: 34290405]
18. Surana U, Amon A, Dowzer C, McGrew J, Byers B, and Nasmyth K (1993). Destruction of the CDC28/CLB mitotic kinase is not required for the metaphase to anaphase transition in budding yeast. EMBO J. 12, 1969–1978. [PubMed: 8491189]

19. Linke C, Chasapi A, González-Novo A, Sawad IA, Tognetti S, Klipp E, Loog M, Krobitsch S, Posas F, Xenarios I, et al. (2017). A Clb/Cdk1-mediated regulation of Fkh2 synchronizes CLB expression in the budding yeast cell cycle. NPJ Syst. Biol. Appl 3, 7–12. [PubMed: 28649434]
20. Palframan WJ, Meehl JB, Jaspersen SL, Winey M, and Murray AW (2006). Anaphase inactivation of the spindle checkpoint. Science 313, 680–684. [PubMed: 16825537]
21. Vernieri C, Chiroli E, Francia V, Gross F, and Ciliberto A (2013). Adaptation to the spindle checkpoint is regulated by the interplay between Cdc28/Clbs and PP2ACdc55. J. Cell Biol 202, 765–778. [PubMed: 23999167]
22. Alexandru G, Zachariae W, Schleiffer A, and Nasmyth K (1999). Sister chromatid separation and chromosome re-duplication are regulated by different mechanisms in response to spindle damage. EMBO J. 18, 2707–2721. [PubMed: 10329618]
23. Amon A, Tyers M, Futcher B, and Nasmyth K (1993). Mechanisms that help the yeast cell cycle clock tick: G2 cyclins transcriptionally activate G2 cyclins and repress G1 cyclins. Cell 74, 993–1007. [PubMed: 8402888]
24. Bishop AC, Ubersax JA, Petsch DT, Matheos DP, Gray NS, Blethrow J, Shimizu E, Tsien JZ, Schultz PG, Rose MD, et al. (2000). A chemical switch for inhibitor-sensitive alleles of any protein kinase. Nature 407, 395–401. [PubMed: 11014197]
25. Edenberg ER, Mark KG, and Toczyski DP (2015). Ndd1 turnover by SCF(Grr1) is inhibited by the DNA damage checkpoint in Saccharomyces cerevisiae. PLoS Genet. 11, e1005162. [PubMed: 25894965]
26. Brandman O, and Meyer T (2008). Feedback loops shape cellular signals in space and time. Science 322, 390–395. [PubMed: 18927383]
27. Örd M, Puss KK, Kivi R, Möll K, Ojala T, Borovko I, Faustova I, Venta R, Valk E, Kõivomägi M, et al. (2020). Proline-Rich Motifs Control G2-CDK Target Phosphorylation and Priming an Anchoring Protein for Polo Kinase Localization. Cell Rep. 31, 107757. [PubMed: 32553169]
28. Kõivomägi M, Valk E, Venta R, Iofik A, Lepiku M, Morgan DO, and Loog M (2011). Dynamics of Cdk1 substrate specificity during the cell cycle. Mol. Cell 42, 610–623. [PubMed: 21658602]
29. Kõivomägi M, Örd M, Iofik A, Valk E, Venta R, Faustova I, Kivi R, Balog ERM, Rubin SM, and Loog M (2013). Multisite phosphorylation networks as signal processors for Cdk1. Nat. Struct. Mol. Biol 20, 1415–1424. [PubMed: 24186061]
30. McGrath DA, Balog ERM, Kõivomägi M, Lucena R, Mai MV, Hirschi A, Kellogg DR, Loog M, and Rubin SM (2013). Cks confers specificity to phosphorylation-dependent CDK signaling pathways. Nat. Struct. Mol. Biol 20, 1407–1414. [PubMed: 24186063]
31. Örd M, and Loog M (2020). Detection of Multisite Phosphorylation of Intrinsically Disordered Proteins Using Phos-tag SDS-PAGE. Methods Mol. Biol 2141, 779–792. [PubMed: 32696389]
32. Goda T, Ishii T, Nakajo N, Sagata N, and Kobayashi H (2003). The RRASK motif in Xenopus cyclin B2 is required for the substrate recognition of Cdc25C by the cyclin B-Cdc2 complex. J. Biol. Chem 278, 19032–19037. [PubMed: 12754270]
33. Cardozo T, and Pagano M (2004). The SCF ubiquitin ligase: insights into a molecular machine. Nat. Rev. Mol. Cell Biol 5, 739–751. [PubMed: 15340381]
34. Berset C, Griac P, Tempel R, Rue JL, Wittenberg C, and Lanker S (2002). Transferable domain in the G(1) cyclin Cln2 sufficient to switch degradation of Sic1 from the E3 ubiquitin ligase SCF(Cdc4) to SCF(Grr1). Mol. Cell. Biol 22, 4463–4476. [PubMed: 12052857]
35. Hsiung YG, Chang HC, Pellequer JL, Valle RL, Lanker S, and Wittenberg C (2001). F-box protein Grr1 interacts with phosphorylated targets via the cationic surface of its leucine-rich repeat. Mol. Cell. Biol 21, 2506–2520. [PubMed: 11259599]
36. Lyons NA, Fonslow BR, Diedrich JK, Yates JR, and Morgan DO (2013). Sequential primed kinases create a damage-responsive phosphodegron on Eco1. Nat. Struct. Mol. Biol 20, 194–201. [PubMed: 23314252]
37. Blondel M, Bach S, Bamps S, Dobbelaere J, Wiget P, Longaretti C, Barral Y, Meijer L, and Peter M (2005). Degradation of Hof1 by SCF(Grr1) is important for actomyosin contraction during cytokinesis in yeast. EMBO J. 24, 1440–1452. [PubMed: 15775961]
38. Quilis I, and Igual JC (2017). A comparative study of the degradation of yeast cyclins Cln1 and Cln2. FEBS Open Bio 7, 74–87.

39. Salama SR, Hendricks KB, and Thorner J (1994). G1 cyclin degradation: the PEST motif of yeast Cln2 is necessary, but not sufficient, for rapid protein turnover. Mol. Cell. Biol 14, 7953–7966. [PubMed: 7969135]
40. Darieva Z, Bulmer R, Pic-Taylor A, Doris KS, Geymonat M, Sedgwick SG, Morgan BA, and Sharrocks AD (2006). Polo kinase controls cell-cycle-dependent transcription by targeting a coactivator protein. Nature 444, 494–498. [PubMed: 17122856]
41. Lim HH, Goh PY, and Surana U (1998). Cdc20 is essential for the cyclosome-mediated proteolysis of both Pds1 and Clb2 during M phase in budding yeast. Curr. Biol 8, 231–234. [PubMed: 9501986]
42. Trcek T, Larson DR, Moldón A, Query CC, and Singer RH (2011). Single-Molecule mRNA Decay Measurements Reveal Promoter-Regulated mRNA Stability in Yeast. Cell 147, 1484–1497. [PubMed: 22196726]
43. Livak KJ, and Schmittgen TD (2001). Analysis of Relative Gene Expression Data Using Real-Time Quantitative PCR and the $2^{-\Delta\Delta C\ T}$ Method. Methods 25, 402–408. [PubMed: 11846609]
44. Puig O, Caspary F, Rigaut G, Rutz B, Bouveret E, Bragado-Nilsson E, Wilm M, and Séraphin B (2001). The tandem affinity purification (TAP) method: a general procedure of protein complex purification. Methods 24, 218–229. [PubMed: 11403571]
45. Reynard GJ, Reynolds W, Verma R, and Deshaies RJ (2000). Cks1 is required for G(1) cyclin-cyclin-dependent kinase activity in budding yeast. Mol. Cell. Biol 20, 5858–5864. [PubMed: 10913169]

Highlights

- As cells enter mitosis, Cdk1 activates and then inhibits mitotic gene expression
- Cdk1 inhibits gene expression in part by promoting degradation of co-activator Ndd1
- Ndd1 degradation is stimulated by Cdk1-mediated phosphorylation at multiple sites
- Multisite Ndd1 phosphorylation depends on phosphate-binding sites in Cks1 and cyclin

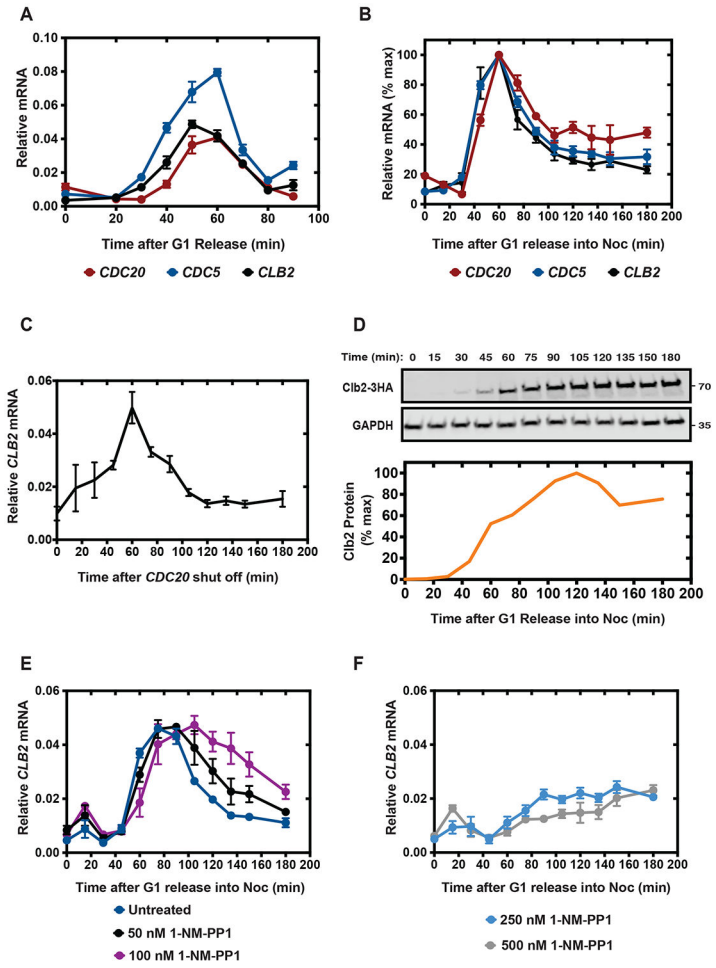

Figure 1. Decline in *CLB2* cluster gene expression in a mitotic arrest depends on Cdk1 activity

(A) Cells were released from a G1 arrest and harvested at the indicated times for analysis of gene expression by RT-qPCR. mRNA for each of the genes was normalized to *ACT1* mRNA. Data points indicate mean +/− S.E.M. in 3 independent experiments.

(B) Gene expression was measured in cells released from G1 arrest into nocodazole (Noc) to induce a mitotic arrest. mRNA for each of the genes was normalized to *ACT1* mRNA. Data points indicate mean +/− S.E.M. in 3 independent experiments.

(C) Cells carrying a replacement of the *CDC20* gene with galactose-inducible *CDC20* were released from a G1 arrest into dextrose to induce a mitotic arrest. *CLB2* expression was measured at the indicated times by RT-qPCR (normalized to *ACT1* mRNA). Data points indicate mean +/− S.E.M. in 3 independent experiments.

(D) Cells were released from G1 into nocodazole. Expression of 3xHA-tagged Clb2 was analyzed by immunoblot at the indicated times, with a GAPDH immunoblot serving as a loading control.

(E & F) Cells carrying analog-sensitive Cdk1 (*cdk1-as1*) were released from G1 arrest into media containing the indicated concentrations of 1-NM-PP1, plus nocodazole. *CLB2* gene expression was measured at the indicated times by RT-qPCR (normalized to *ACT1* mRNA). Data points indicate mean +/− S.E.M. in 3 independent experiments.

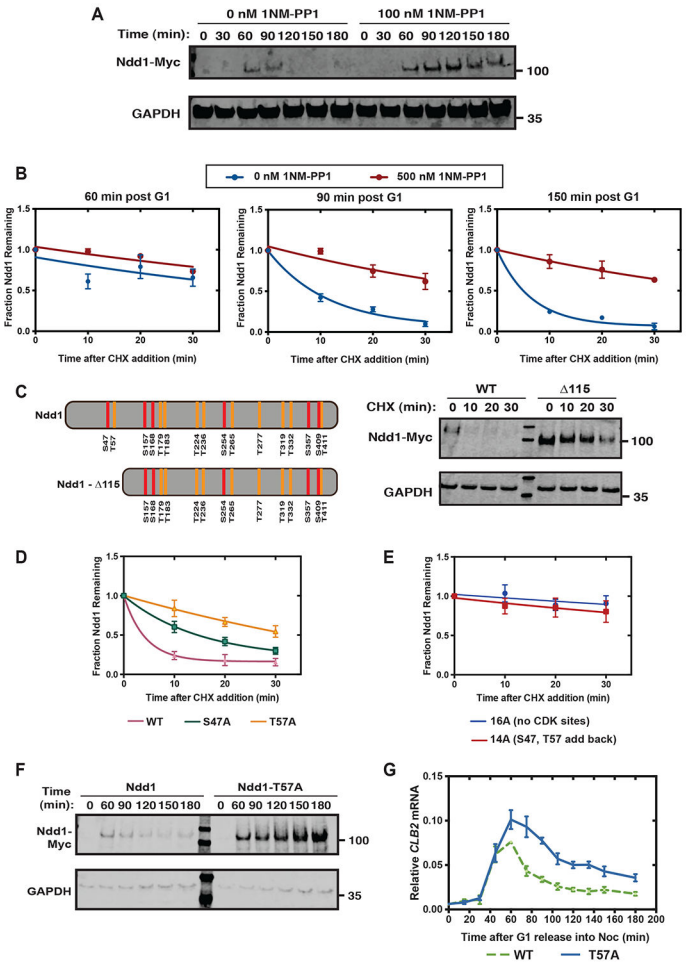

Figure 2. Ndd1 destabilization depends on rising Cdk1 activity and N-terminal phosphorylation

(A) *cdk1-as1* cells carrying Myc-tagged Ndd1 at the endogenous *NDD1* locus were released from a G1 arrest into nocodazole in the absence (left) or presence (right) of 100 nM 1-NM-PP1. Myc-tagged Ndd1 and GAPDH expression were monitored by immunoblot at the indicated times. See Figure S1A for analysis in wild-type cells.

(B) Parallel cultures of *cdk1-as1* cells carrying Myc-tagged Ndd1 at the endogenous *NDD1* locus were released from a G1 arrest into nocodazole. Cycloheximide (CHX) was added after 60, 90, or 150 min. 500 nM 1-NM-PP1 was added with CHX in parallel cultures. Samples were harvested after 0, 10, 20, or 30 min in CHX. Ndd1-Myc levels were analyzed by immunoblot and quantified. Data points indicate mean +/− S.E.M. in 2 independent experiments. Curves were generated by fitting data to a single exponential decay model.

(C) *Left:* Depiction of Ndd1 and an Ndd1 mutant lacking the first 115 amino acids (Ndd1-Δ115), with 16 consensus Cdk1 sites marked (serine, red; threonine, orange). See Figure S2 for Ndd1 sequence. *Right:* Cells carrying galactose-inducible wild-type (WT) Ndd1 or Ndd1-Δ115 were grown in galactose and arrested in mitosis with nocodazole. CHX was added, and Ndd1-Myc and GAPDH were analyzed by immunoblotting at the indicated times.

(D) Cells carrying galactose-inducible Ndd1 (WT), Ndd1-S47A, or Ndd1-T57A were treated as in panel C. Quantification of immunoblots from 3 independent experiments (mean

+/− S.E.M.). Curves were generated by fitting data to a single exponential decay model. Representative immunoblot in Figure S1B.

(E) Cells carrying Ndd1-16A or Ndd1 containing only S47 and T57 (Ndd1-14A) were treated as in panel C. Quantification of immunoblots from 3 independent experiments (mean +/− S.E.M.). Curves were generated by fitting data to a single exponential decay model. Representative immunoblot in Figure S1C.

(F) Cells carrying Myc-tagged WT Ndd1 or Ndd1-T57A at the endogenous *NDD1* locus were released from a G1 arrest into nocodazole to induce a mitotic arrest. Ndd1-Myc and GAPDH levels were analyzed by immunoblotting at the indicated times.

(G) Cells carrying WT Ndd1 or Ndd1-T57A as in panel F were released from G1 arrest into nocodazole. Samples were harvested at the indicated times for analysis of *CLB2* gene expression by RT-qPCR (normalized to *ACT1* mRNA). Dashed line indicates data for WT from Figure 1B. Data points indicate mean +/− S.E.M. in 3 independent experiments.

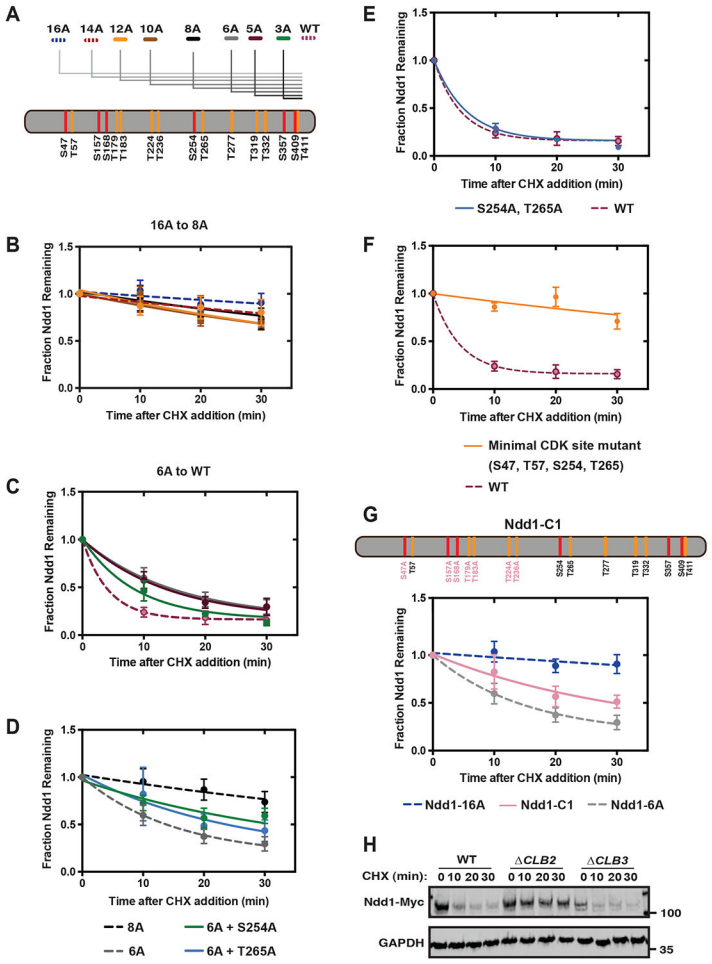

Figure 3. Multiple predicted Cdk1 sites promote Ndd1 destabilization

(A) Diagram of predicted Cdk1 sites in Ndd1, showing the sites mutated to alanine in the Ndd1 mutants analyzed in panels B and C. See Figure S2 for Ndd1 sequence.

(B) Cells carrying galactose-inducible Ndd1 alanine mutants 12A, 10A, or 8A (colors indicated in panel A) were grown in galactose and arrested in mitosis with nocodazole. CHX was added, and Ndd1-Myc was quantified by immunoblotting at the indicated times. Data points indicate mean +/− S.E.M. in 3 independent experiments. Dashed lines indicate data for Ndd1-16A and Ndd1-14A from Figure 2E.

(C) Cells carrying galactose-inducible Ndd1 alanine mutants 6A, 5A, or 3A were treated and analyzed as in panel B. Data points indicate mean +/− S.E.M. in 3 independent experiments. Dashed line indicates data for WT Ndd1 from Figure 2D.

(D) Cells were constructed in which galactose-inducible Ndd1 carried alanine mutations at the C-terminal six Cdk1 consensus sites (Ndd1-6A; see panel A) plus a mutation of either S254 or T265 to alanine, and were treated as in panel B. Quantification of immunoblots from 3 independent experiments (mean +/− S.E.M.). Dashed lines indicate data for Ndd1-8A and Ndd1-6A from panels B and C, respectively. Representative immunoblot in Figure S3A.

(E) Cells carrying galactose-inducible Ndd1-S254A, T265A were treated and analyzed as in panel B. Quantification of immunoblots from 3 independent experiments (mean +/− S.E.M.).

Dashed line indicates data for WT Ndd1 from Figure 2D. Representative immunoblot in Figure S3B.

(F) Cells were constructed in which galactose-inducible Ndd1 carried alanine mutations at all Cdk1 consensus sites except S47, T57, S254, and T265. Cells were treated and analyzed as in panel B. Quantification of immunoblots from 3 independent experiments (mean +/− S.E.M.). Dashed line indicates data for WT Ndd1 from Figure 2D. Representative immunoblot in Figure S3C.

(G) Cells carrying galactose-inducible Ndd1 containing only T57, S254, T265, T277, T319, T332, S357, S409, and T411 (Ndd1-C1) were treated and analyzed as in panel B. Quantification of immunoblots from 3 independent experiments (mean +/− S.E.M.). Dashed lines indicate data for Ndd1-16A and Ndd1-6A from Figure 2E and panel C, respectively. Representative immunoblot in Figure S3D.

(H) Cells expressing galactose-inducible Ndd1-Myc were arrested in mitosis with nocodazole. CHX was added, and Ndd1-Myc and GAPDFI were analyzed by immunoblotting at the indicated times.

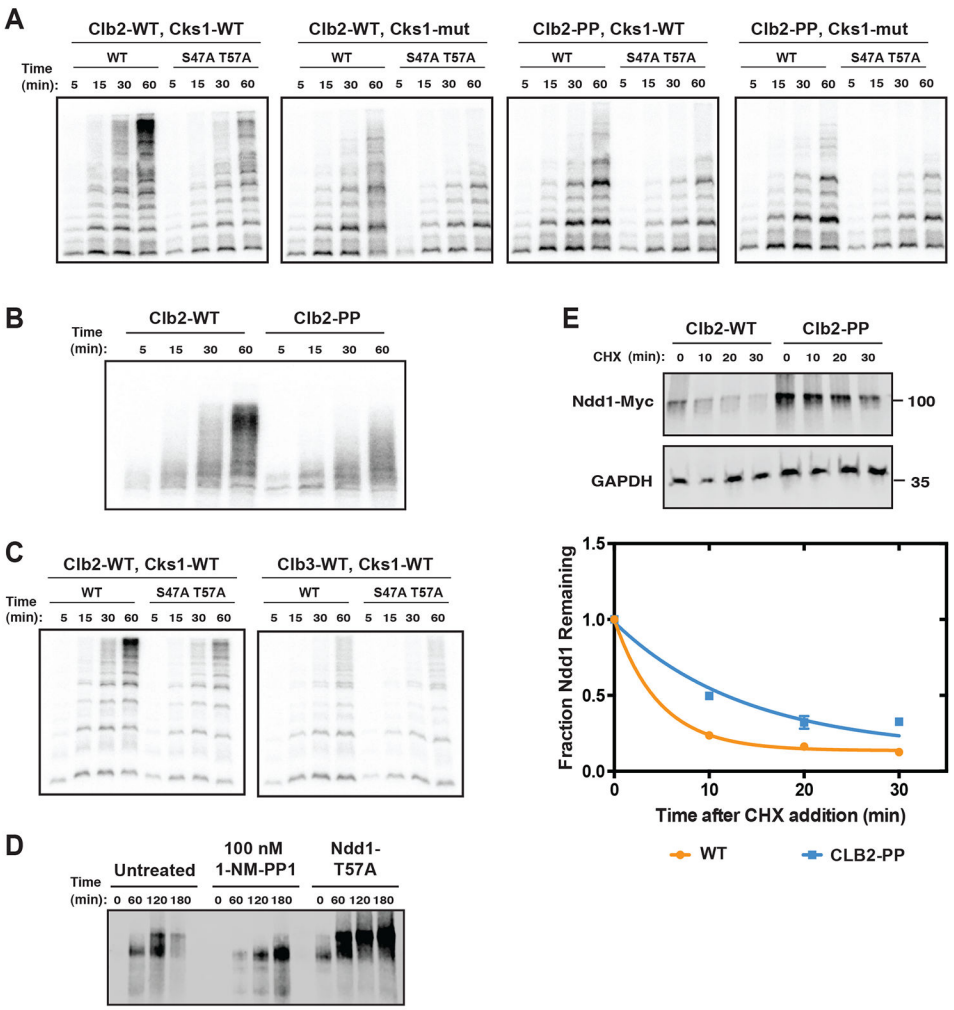

Figure 4. N-terminal phosphorylation of Ndd1 depends on phosphate-binding pockets of Cks1 and Clb2

(A) Truncated Ndd1 (aa 1-272), either wild-type (WT) or S47A T57A, was incubated with [γ-^{32}P]-ATP and the indicated Clb2-Cdk1-Cks1 complex: panel 1: wild-type complex; panel 2: a complex containing Cks1 with mutations in the phosphothreonine-binding site (R33E S82E R102A; Cks1-mut); panel 3: a complex containing Clb2 with mutations in the phosphate-binding pocket (R366A R379A K383A; Clb2-PP); panel 4: a complex containing mutations in both Cks1 and Clb2. Reactions were stopped at the indicated times, and reaction products were analyzed by Phos-tag SDS-PAGE and autoradiography. Results are representative of three independent experiments. See Figure S4 for mass spectrometry analysis of Ndd1 phosphorylation sites.

(B) Full-length Ndd1-WT was incubated with [γ-^{32}P]-ATP and wild-type (WT) Clb2-Cdk1-Cks1 or with a complex containing Clb2-PP. Reactions were analyzed as in panel A. Results are representative of two independent experiments.

(C) Truncated Ndd1 (aa 1-272), either wild-type (WT) or S47A T57A, was incubated with [γ-^{32}P]-ATP and either Clb2-Cdk1-Cks1 (left) or Clb3-Cdk1-Cks1 (right). Reactions were analyzed as in panel A. Results are representative of two independent experiments.

(D) *cdk1-as1* cells carrying Myc-tagged wild-type Ndd1 (left 8 lanes), or wild-type cells carrying Myc-tagged Ndd1-T57A (right 4 lanes), were released from a G1 arrest into nocodazole. As indicated, some cells were treated with 100 nM 1-NM-PP1 to inhibit Cdk1 activity. Levels and phosphorylation of Ndd1 were assessed by Phos-tag SDS-PAGE and immunoblotting.

(E) A strain was constructed in which the *CLB2* locus was replaced with a mutant gene encoding Clb2-PP. Cells carrying galactose-inducible Ndd1-Myc were grown in galactose and arrested in mitosis with nocodazole. CHX was added, and Ndd1-Myc was analyzed by immunoblotting at the indicated times. Top panel shows a representative immunoblot. Bottom panel shows quantification of Ndd1 from four independent experiments (mean +/− S.E.M.).

KEY RESOURCES TABLE

REAGENT or RESOURCE	SOURCE	IDENTIFIER
Bacterial and Virus Strains		
E. coli BL21-CodonPlus(DE3)-RP	Agilent Technologies	Cat# 230255
Antibodies		
Myc-Tag (9B11) Mouse mAb	Cell Signaling Technology	Cat# 2276; RRID:AB_331783
HA-Tag (12CA5) Mouse mAb	Sigma	Cat# 11 583 816 001; RRID:AB_2532070
Rabbit anti-Mouse IgG (H+L) Alexa Fluor 680	Thermo Fisher Scientific	Cat# A-21065; RRID:AB_2535728
GAPDH Monoclonal Antibody (GA1R)	Thermo Fisher Scientific	Cat# MA5-15738; RRID:AB_10977387
IRDye®800CW Donkey anti-Mouse IgG Secondary Antibody	Licor	Cat# 926-32212 RRID:AB_2716622
Chemicals, peptides, and recombinant proteins		
TURBO DNase	Thermo Fisher Scientific	Cat# AM1907
4-20% Mini-PROTEAN® TGX™ Precast Protein Gels	BioRad	Cat# 4561096
Phostag Reagent	Wako Chemicals	Cat# AAL-107M
[γ-^{32}P]-ATP	Hartmann Analytic	Cat# SRP-501
[O^{18}]-ATP	Cambridge Isotope Laboratories, Inc	Cat# OLM-7858-20
C18 StageTips	Sigma	Cat# 66883-U
alpha-factor Mating Pheromone, yeast	Genscript	Cat#: RP01002
1NM-PP1 (PP1 Analog II)	Sigma	Cat#: 529581-1MG
Nocodazole	Sigma	Cat#: M1404-50MG
Cycloheximide	Sigma	Cat#: 01810-5G
Galactose	US Biological	Cat# 211820
Dextrose	US Biological	Cat# G3050
Yeast Extract	BD Biosciences	Cat# 212720
Peptone	BD Biosciences	Cat# 211820
Purified Ndd1 and Ndd1(1-272)	This study	N/A
Purified Clb2-Cdk1-Cks1 and Clb3-Cdk1-Cks1	This study	N/A
Critical commercial assays		
Luna® Universal One-Step RT-qPCR reaction	NEB	Cat# E3005L
Experimental models: Organisms/strains		
Wild-type W303: *MATa, bar1::HisG*	ATCC	DOM0090
cdc20::LEU2 trp1::GAL-CDC20-TRP1	[41]	DOM0268
CLB2-3XHA:HIS3MX6	[3]	DOM0948
cdc28::cdc28-as1	[24]	DOM0030
ndd1::NDD1-9xMYC-HYGR	This study	JBA073

REAGENT or RESOURCE	SOURCE	IDENTIFIER
cdc28::CDC28-as1 ndd1::NDD1-9xMYC-HYGR	This study	JBA072
clb2::KANMX trp1::pGAL-NDD1-9XMYC-TRP1	This study	JBA058
clb3::KANMX trp1::pGAL-NDD1-9XMYC-TRP1	This study	JBA059
trp1::pGAL-Δ1-115-NDD1-9XMYC-TRP1	This study	JBA004
trp1::pGAL-NDD1-S47A-9XMYC-TRP1	This study	JBA060
trp1::pGAL-NDD1-T57A-9XMYC-TRP1	This study	JBA055
trp1::pGAL-NDD1-S47A-T57A-S157A-S168A-T179A-T183A-T224A-T236A-S254A-T265A-T277A-T319A-T332A-S357A-S409A-T411A-9XMYC-TRP1	This study	JBA074
trp1::pGAL-NDD1-S157A-S168A-T179A-T183A-T224A-T236A-S254A-T265A-T277A-T319A-T332A-S357A-S409A-T411A-9XMYC-TRP1	This study	JBA075
trp1::pGAL-NDD1-T179A-T183A-T224A-T236A-S254A-T265A-T277A-T319A-T332A-S357A-S409A-T411A-9XMYC-TRP1	This study	JBA001
trp1::pGAL-NDD1-T224A-T236A-S254A-T265A-T277A-T319A-T332A-S357A-S409A-T411A-9XMYC-TRP1	This study	JBA006
trp1::pGAL-NDD1-S254A-T265A-T277A-T319A-T332A-S357A-S409A-T411A-9XMYC-TRP1	This study	JBA043
trp1::pGAL-NDD1-T277A-T319A-T332A-S357A-S409A-T411A-9XMYC-TRP1	This study	JBA033
trp1::pGAL-NDD1-T319A-T332A-S357A-S409A-T411A-9XMYC-TRP1	This study	JBA042
trp1::pGAL-NDD1-S357A-S409A-T411A-9XMYC-TRP1	This study	JBA054
trp1::pGAL-NDD1-T265A-T277A-T319A-T332A-S357A-S409A-T411A-9XMYC-TRP1	This study	JBA063
trp1::pGAL-NDD1-S254A-T277A-T319A-T332A-S357A-S409A-T411A-9XMYC-TRP1	This study	JBA061
trp1::pGAL-NDD1-S254A, T265A-9XMYC-TRP1	This study	JA062
trp1::pGAL-NDD1-S157A-S168A-T179A-T183A-T224A-T236A-T277A-T319A-T332A-S357A-S409A-T411A-9XMYC-TRP1	This study	JBA070
trp1::pGAL-NDD1-S47A-S157A-S168A-T179A-T183A-T224A-T236A-9XMYC-TRP1	This study	JBA068
trp1::pNDD1-NDD1-T57A-9XMYC	This study	JBA056
ndd1::HYGR trp1::pNDD1-NDD1-T57A	This study	JBA046
trp1::pGal-NDD1 clb2::CLB2-R336A, R379A, K383A - HYGR	This study	JBA071
bar1Δ::HISG sic1Δ::LEU2 pRS426-GAL1-CLB2-TAP	[1]	N/A
bar1Δ::HISG sic1Δ::LEU2 pRS426-GAL1-CLB3-TAP	[6]	N/A
bar1Δ::HISG sic1Δ::LEU2 pRS426-GAL1-CLB2(R366A R379A K383A)-TAP	This study	N/A
Oligonucleotides		
CLB2 FWD: GGTATCCAACTCCCCAAAAACAATCTTTTAG	This study	N/A
CLB2 REV: CGAGTTATGGACTACCTCAGTGCTTGATC	This study	N/A
ACT1 FWD: GATAACGGTTCTGGTATGTGTAAAGCC	This study	N/A
ACT1 REV: GTGACAATACCGTGTTCAATTGGGTAA	This study	N/A

REAGENT or RESOURCE	SOURCE	IDENTIFIER
CDC5 FWD: CGTGAAGCAAGGATACGTAGAG	This study	N/A
CDC5 REV: GGAGAACTGTGGTGCCATTAT	This study	N/A
CDC20 FWD: GATCCCAGGTGAGCTCTTTAC	This study	N/A
CDC20REV: CCATCCATCAATCCGTCTTCT	This study	N/A
Recombinant DNA		
pMO818, 6xHis-Ndd1 pET28a	This study	N/A
pMO1020, 6xHis-Ndd1(1-272) pET28a	This study	N/A
6xHis-Ndd1(1-272 S47A T57A) pET28a	This study	N/A
pCKS1	[6]	N/A
pCKS1-mut	[6]	N/A
Software and algorithms		
ImageQuant TL Version 8.1	Cytiva	https://www.cytivalifesciences.com/en/us/shop/protein-analysis/molecular-imaging-for-proteins/imaging-software/imagequant-tl-8-1-p-00110
ImageStudioLite Version 5.2.5	LI-COR	https://www.licor.com/bio/image-studio-lite/
Prism Version 9.2.0	Graphpad	https://www.graphpad.com/scientific-software/prism/
Mascot Version 2.3	Matrix Science	https://www.matrixscience.com